

# Multi-Objective Parametric Optimization Design for Mirrors Combined with Non-Dominated Sorting Genetic Algorithm

Lu Sun <sup>1,2,\*</sup>, Bao Zhang <sup>1,2</sup>, Ping Wang <sup>1</sup>, Zhihong Gan <sup>1</sup>, Pengpeng Han <sup>1</sup> and Yijian Wang <sup>1,2</sup>

<sup>1</sup> Key Laboratory of Airborne Optical Imaging and Measurement, Changchun Institute of Optics, Fine Mechanics and Physics, Chinese Academy of Sciences, Changchun 130033, China

<sup>2</sup> University of Chinese Academy of Sciences, Beijing 100049, China

\* Correspondence: sunlu\_ciomf@163.com

**Abstract:** The process of intelligent multi-objective parametric optimization design for mirrors is discussed in detail in this paper, with the error of the mirror surface shape and the total mass being examined as the optimization objectives. The establishment of complex objective functions for solving the optimization problem of the mirror surface shape error was realized, and manual modification of the model was avoided. Moreover, combining this with a non-dominated sorting genetic algorithm (NSGA) helped the Pareto front move towards an ideal optimal set of solutions. To verify the effectiveness of the proposed method, an aluminum alloy mirror with an aperture of 140 mm was taken as an example. The Pareto optimal solution set of the mass and surface shape error under 1 g gravity was obtained for finding the required solution and satisfying the optimization goal. In addition, this method is applicable to other complex structural design problems.

**Keywords:** intelligent parameter optimization design; joint simulation; non-dominated sorting genetic algorithm; mirror surface shape error; Pareto optimal solution set



**Citation:** Sun, L.; Zhang, B.; Wang, P.; Gan, Z.; Han, P.; Wang, Y. Multi-Objective Parametric Optimization Design for Mirrors Combined with Non-Dominated Sorting Genetic Algorithm. *Appl. Sci.* **2023**, *13*, 3346. <https://doi.org/10.3390/app13053346>

Academic Editors: Andrés Márquez and Paolo Renna

Received: 30 December 2022

Revised: 21 February 2023

Accepted: 28 February 2023

Published: 6 March 2023



**Copyright:** © 2023 by the authors. Licensee MDPI, Basel, Switzerland. This article is an open access article distributed under the terms and conditions of the Creative Commons Attribution (CC BY) license (<https://creativecommons.org/licenses/by/4.0/>).

## 1. Introduction

The analysis of rigid-body motion and surface shape errors in mirror design problems plays an important role in evaluating the environmental adaptability, spatial position stability and imaging quality of opto-mechanical structures [1–3]. Usually, the root mean square value (RMS) of a mirror's surface shape error is used to verify whether the structural design meets the optical imaging requirements. It is worth noting that among the components of a mirror's surface shape error resulting from its own weight, rigid-body motion, which represents the translation and tilt of the mirror, could be eliminated by recalibrating the optical system. Therefore, rigid-body motion needs to be removed from a mirror's surface shape error while describing the mirror's surface shape quality.

During the actual mirror design process, the structure is often modeled first and is subsequently simulated and analyzed in finite-element software for obtaining the node deformation on the mirror's surface, and then the results are exported for further processing to calculate the surface shape error. There are two main kinds of methods that are used to separate the rigid-body motion of the mirror from the surface shape error. One involves taking an accurate fitting for deformed surface shapes using Zernike polynomials [4]. The second involves the surface equation processing method proposed by Wu et al. [5]. The traditional design relies more on experience. If the surface shape error exceeds the requirements, the designer needs to change the model parameters manually, and then the above simulation and processing procedure needs to be repeated several times until the results meet the requirements. As we can see, the whole design process always requires manual repetitive work, and, furthermore, the results often likely do not provide the optimal solution.

With the development of finite-element software, many engineering designers have used this optimization design software to optimize the structure of mirrors, including

size optimization, topology optimization and shape optimization [6]. There have been a lot of studies on about mirror optimization using different kinds of software. Park k.S. et al. [7] studied the optimization of the topology of a primary mirror under its own weight and polishing loading, where the measure of the Strehl ratio was used to perform the objective function, thus establishing the relationship between the optical surface quality and node deformation. The structural optimization of a 1.2 m diameter space mirror using the OptiStruct tool from HyperWorks 12 to minimize the mass and constrain optical aberrations was carried out by Sahu et al. [8]. Qu et al. [9] also used OptiStruct to optimize the topology of a lightweight primary mirror assembly to determine its shape, and then the sensitivity analysis method and size optimization were adopted to determine the structural parameters. A parametric optimization method to design large, lightweight space mirrors based on the optimization of the topology of a basic mirror configuration was proposed by Liu et al. [2], which combined the advantages of topology optimization and parametric optimization. The whole optimization process involved the Isight software, OptiStruct and the MATLAB software. Their study implies that optimization software could be effectively used to address mirror optimization. However, the following limitations exist for designers: (1) it takes a long time to learn and figure out the software's functions, and usually it is not easy to get started if you are not familiar with optimization design software; (2) the built-in optimization algorithms are fixed and are difficult to modify; (3) in optimization design software, usually only one objective function can be set. To achieve multi-objective optimization, the weights need to be introduced to transform the multi-objective optimization problem into a single-objective optimization problem. The choice of weights involves a subjective judgment from the designer.

Different from optimization software, the method proposed in this study realizes the whole optimization process by using MATLAB-Python-Abaqus joint simulation, which can provide a more flexible and convenient way to achieve structural parametric optimization design, especially for people who are good at programming. This method has advantages in terms of multi-objective optimization and complex objective function implementation, focusing on the needs of designers more closely. In addition, the combination of this with a non-dominated sorting genetic algorithm achieves intelligent variable parameter optimization design and helps the Pareto front to quickly move towards the ideal optimal set of solutions.

## 2. Optimization Method

### 2.1. Optimization Implementation

The whole process involves a multi-objective optimization algorithm program, a finite-element simulation and data interaction among different pieces of software. It is well known that MATLAB has a powerful programming function and numerical computation ability, while Abaqus has powerful finite-element modeling and simulation functions. This optimization method combines the powerful functions of these two pieces of software to realize the structural parameter optimization. Since the kernel language of Abaqus is Python and Python languages can be conveniently run by MATLAB, Python is necessary for realizing the data interaction between them. Specifically, extracting the data from the results database of Abaqus as well as rewriting the modelling file with different values of the structural parameters are completed via Python codes.

In this paper, the main program is implemented through MATLAB (MathWorks Inc., R2017a, Natick, MA, USA), and a non-dominated sorting genetic algorithm is used as the multi-objective optimization algorithm. The population consisted of mirror structure optimization parameters, and the chromosome length is determined according to the number of optimization parameters and constraints. When calculating the objective values corresponding to the individuals, the relevant structural parameters are obtained based on these different individuals by converting the binary values into decimal values, and then the values are assigned to the corresponding parameters in the modeling file to update the model into the Python language (Python Software Foundation. Python Language

Reference, version 3.4.0 Available at <http://www.python.org>, accessed on 17 March 2014). Subsequently, Abaqus (Dassault Systèmes Simulia Corp., Version 6.9, Paris, France) is called upon to perform the simulation calculations, and the results are then obtained, which are further processed to obtain the corresponding objective values. In each generation, the optimal individuals and the optimal objective values are acquired with the non-dominated sorting method. After this, the next generation population is obtained through selection, crossover and mutation operations, and then the process of calculating the objective values is repeated. After multiple iterations, the final solution set consisting of the optimal objective values are obtained, and this is the Pareto optimal solution set. Accordingly, the designer may select the most suitable optimization result. The optimization flowchart and data interaction diagram are shown in Figures 1 and 2, respectively.

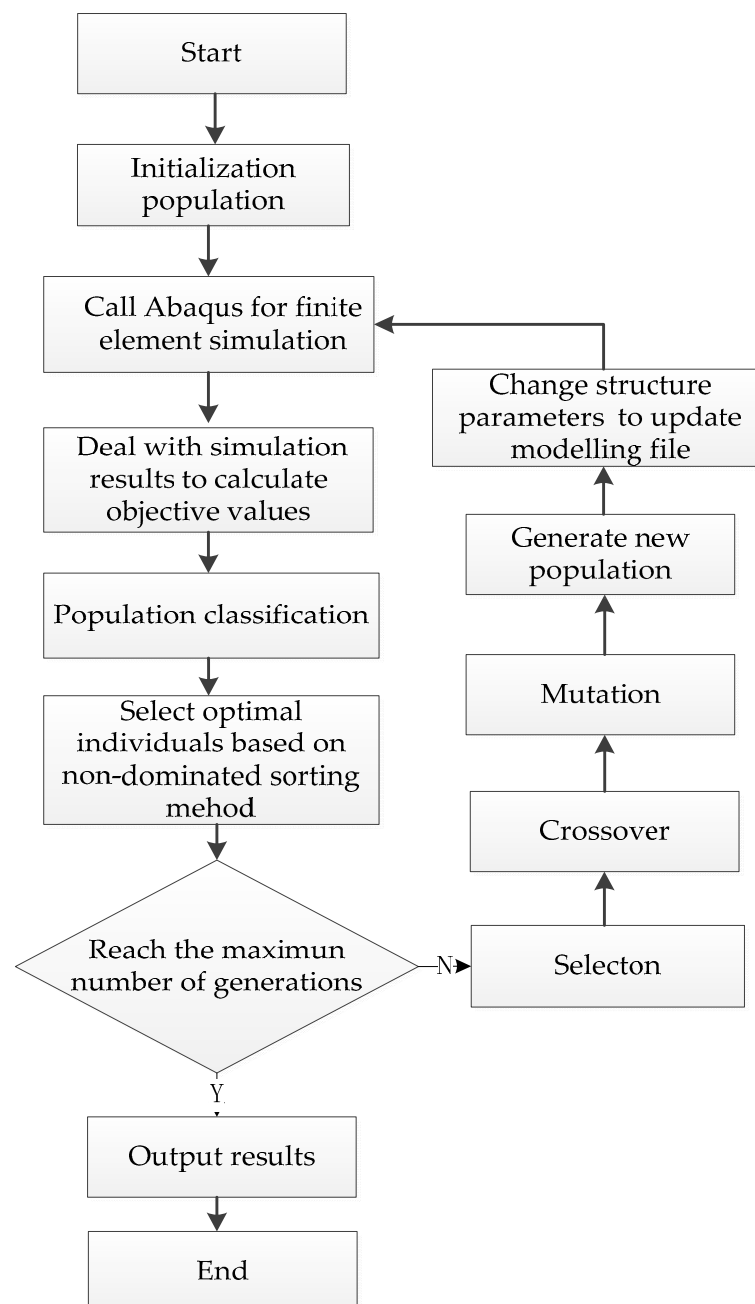


**Figure 1.** Optimization flowchart.

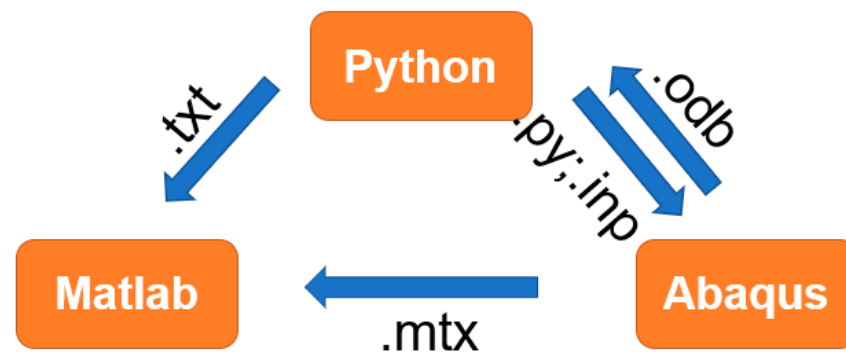


**Figure 2.** Data interaction diagram.

The main steps are as follows:

1. Determine the optimization parameters, constraints and objective functions for the optimization problem;
2. Generate the modelling file by using the recording macro file function of Abaqus or scripting the file directly to model the structure, divide the mesh, define the material properties, determine the cell type, establish the analysis step, apply the load and boundary conditions, and submit the computation process;
3. Write codes for extracting the required data from the results database of Abaqus and then input these codes following up those in the above modelling file. Up to this point, the modelling file may complete the whole process of simulating the deformation for the mirror model with the determined structural parameters;
4. Run the modelling file in Abaqus and save the results;
5. Input the results into the objective function to calculate the objective values for population classification. According to the non-dominated sorting method, the Pareto optimal individuals are then selected for this generation;
6. Retain the optimal individuals and input them into the next generation population. Meanwhile, perform the crossover and mutation operations on the old population to obtain the new generation population;
7. By converting binary values to decimal values, the new optimization parameters are generated based on the new population. Then, rewrite the modelling file in Python codes to assign the new optimization parameters of the structure;
8. Repeat steps (iv)–(vii) until the number of generations is satisfied;
9. Output the overall Pareto optimal solution set and pick the multi-objective optimal solution according to the demand.

## 2.2. Non-Dominated Sorting Genetic Algorithm

Non-dominated sorting genetic algorithms (NSGA), which were proposed by Srinivas and Deb [10] in 1995, are genetic algorithms based on the concept of a Pareto optimum and are an improvement on basic genetic algorithms and are performed on the basis of the selection and regeneration method; each individual is classified according to their dominant and non-dominant relations and then the selection operation is conducted, which thus leads to very satisfactory results when conducting multi-objective optimization. With the development of NSGAs, Deb et al. proposed a fast non-dominated sorting genetic algorithm with an elite strategy (NSGA-II) [11,12] in 2000, which can preserve the solution's diversity. However, it has the disadvantages of slow convergence and falling into a local optimum [13]. With the application of the NSGA-II algorithm to a wider range, these problems have gradually emerged. Many researchers have been devoted to improving the NSGA-II algorithm by introducing advanced strategies, such as the random walk strategy for local searching, the Levy flight strategy for global searching [14] or by combining it with other advanced algorithms [15]. Subsequently, the non-dominated sorting genetic algorithm III (NSGA-III) [16] was developed for cases when there are more than four

objectives to be optimized and where it is difficult to select the Pareto solutions. The basic process is similar to that of the NSGA-II algorithm, but the method of selecting individuals incorporates a reference-point-based approach, which can effectively reduce the computational costs and maintain a good diversity of the population. It also uses a niching algorithm rather than the crowding distance method used in the NSGA-II algorithm to make the optimal solution be more evenly distributed in space. Therefore, it shows a better diversity and convergence than the NSGA-II algorithm. For actual engineering problems, there are usually two–three objectives that need to be optimized. Thus, the NSGA-II algorithm is the most popular multi-objective optimization algorithm developed so far, and it has a wide range of applications [17–20].

The core of the NSGA, NSGA-II and NSGA-III algorithms is the non-dominated sorting method. For minimization problems in multi-objective optimization, the objective vector consists of  $n$  subobjectives, i.e.,  $\bar{f}(\mathbf{X}) = (f_1(\mathbf{X}), f_2(\mathbf{X}), \dots, f_n(\mathbf{X}))$ .

For any variables  $\mathbf{X}_p$  and  $\mathbf{X}_q$ ,

1.  $\mathbf{X}_p$  dominates  $\mathbf{X}_q$  if and only if for  $\forall i \in \{1, 2, \dots, n\}, f_i(\mathbf{X}_p) < f_i(\mathbf{X}_q)$ ;
2.  $\mathbf{X}_p$  weakly dominates  $\mathbf{X}_q$  if and only if for  $\forall i \in \{1, 2, \dots, n\}, f_i(\mathbf{X}_p) \leq f_i(\mathbf{X}_q)$  and there exists  $j \in \{1, 2, \dots, n\}$  such that  $f_j(\mathbf{X}_p) < f_j(\mathbf{X}_q)$ ;
3.  $\mathbf{X}_p$  and  $\mathbf{X}_q$  do not dominate each other if and only if for  $\exists i \in \{1, 2, \dots, n\}, f_i(\mathbf{X}_p) < f_i(\mathbf{X}_q)$  and also  $\exists j \in \{1, 2, \dots, n\}$  such that  $f_j(\mathbf{X}_p) > f_j(\mathbf{X}_q)$ .

If there is no solution that dominates  $\mathbf{X}_p$ , then  $\mathbf{X}_p$  is known as the Pareto optimal solution. The set of all the Pareto optimal solutions is the Pareto optimal solution set. The mapping of the Pareto optimal solution set in the objective space is called the Pareto front.

Due to the advantages of NSGAs in multi-objective optimization problems, there are many examples of their application in opto-mechanical structure optimization problems, especially in the parametric optimization area. Mikio Kunita [21] et al. applied a genetic algorithm to the main support structure of a space camera in order to achieve a lightweight design. Hangyong Kihm and Ho. Soon Yang proposed a design process for a main mirror and its flexible support structure and used a genetic algorithm to optimize its design, which met the design requirements and reduced the time consumed by an order of magnitude [22,23]. Liu et al. realized the parametric optimization design of a mirror by using the NSGA-II algorithm [2]. Zhang et al. proposed a recurrent neural network prediction model based on the Bayesian regularization algorithm for an optical–mechanical system, and the NSGA-II algorithm was used to globally optimize the multiple prediction objectives of the prediction model [24].

### 2.3. Rigid-Body Motion and Surface Shape Error of a Mirror

In this paper, the surface equation processing method and the best fit by the least-squares method [5,25–27] were adopted to calculate the rigid-body motion for an optical surface with multiple nodes based on area-weighted average motion. As is well known, the rigid-body motion of an optical surface includes six components (three translations,  $T_x, T_y, T_z$ , and three rotations,  $R_x, R_y, R_z$ ), and the nodal rigid-body displacements,  $d_{\tilde{x}_i}, d_{\tilde{y}_i}, d_{\tilde{z}_i}$ , generated at a given node,  $x_i, y_i, z_i$ , can be expressed as follows:

$$\begin{cases} d_{\tilde{x}_i} = T_x - z_i R_y - y_i R_z \\ d_{\tilde{y}_i} = T_y - z_i R_x - x_i R_z \\ d_{\tilde{z}_i} = T_z - y_i R_x - x_i R_y \end{cases} \quad (1)$$

The squared difference,  $E$ , between the actual nodal displacements,  $d_{x_i}, d_{y_i}, d_{z_i}$ , and the nodal rigid-body displacements,  $d_{\tilde{x}_i}, d_{\tilde{y}_i}, d_{\tilde{z}_i}$ , of an optical surface can be obtained as follows:

$$E = \sum_i \left[ (d_{x_i} - d_{\tilde{x}_i})^2 + (d_{y_i} - d_{\tilde{y}_i})^2 + (d_{z_i} - d_{\tilde{z}_i})^2 \right] \quad (2)$$

For Equation (2), by taking the partial derivatives of each of the six rigid-body motion components, the squared difference,  $E$ , on the left side is zero. Thus, six simultaneous

equations for solving the average rigid-body motion are obtained. After getting the average rigid-body motion of the surface, the rigid-body motion components can be removed from the actual nodal displacements by using Equation (3). Thus, the deformation of each node ( $\Delta_{x_i}, \Delta_{y_i}, \Delta_{z_i}$ ) on the surface of the mirror can be obtained.

$$\begin{aligned} \Delta_{x_i} &= d_{x_i} - d_{\tilde{x}_i} \\ \Delta_{y_i} &= d_{y_i} - d_{\tilde{y}_i} \\ \Delta_{z_i} &= d_{z_i} - d_{\tilde{z}_i} \end{aligned} \tag{3}$$

Furthermore, the error of the mirror deformation relative to the ideal mirror surface can be obtained, and the root mean square value (RMS) of the error can be calculated. Using the above method, the root mean square values of the surface shape error in three directions can be conveniently obtained.

### 3. Mirror Optimization Design

#### 3.1. Fundamental Structure of a Mirror

The choice of the diameter–thickness ratio of a mirror will affect not only the mirror deformation but also the lightweight rate. According to the relationship between the thickness ratio of a flat solid mirror with a circular edge and the self-weight deformation of the mirror, as shown in References [28–30], the diameter-to-thickness ratio of the mirror is preliminarily determined. The empirical equation is as follows:

$$\delta = \frac{3\rho g R^4}{16Et^2} = \frac{3\rho g \Delta^2 D^2}{256E} \tag{4}$$

where  $\delta$  ( $\mu\text{m}$ ) is the maximum deformation of the mirror,  $\rho$  ( $\text{kg}/\text{m}^3$ ) is the material density,  $R$  (m) is the half-diameter of the mirror aperture,  $E$  (GPa) is the elastic modulus of the material,  $t$  (m) is the mirror thickness,  $\Delta$  is the diameter-thickness ratio and  $g$  is the acceleration due to gravity. Aluminum alloy 6061 was selected as the material of the mirror in this study. The mirror aperture was 140 mm. For a value of  $\delta$  of 0.004  $\mu\text{m}$ , the diameter–thickness ratio  $\Delta$  is 6.72, and the mirror thickness  $t$  is 20.83 mm. The support form refers to the method mentioned in Reference [28]. Similar to a single-arch support form, this support form is simple and easy to implement for small-aperture mirrors, as shown in Figure 3. Here, the Z-axis direction was set as the direction of the optical axis, the direction of the Y-axis was set against gravity and the X-axis direction was determined by the rules of the Cartesian coordinate system.

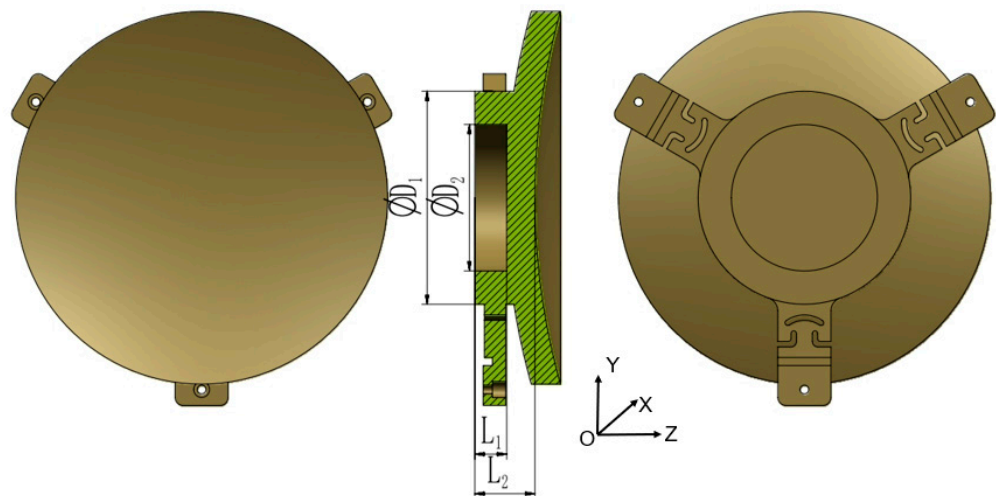


Figure 3. Fundamental structure of the mirror.

### 3.2. Optimization Problem Construction

In addition to the mirror's surface shape error, the mass of the mirror is also something to be considered. Thus, the mass and RMS value of the surface shape error were selected as the optimization objectives. Considering that the mirror as one part of the optical system was mounted on an aerial platform, the altitude of the mirror changed with the platform altitude and the rotation of the gimbal system during working process; therefore, the average RMS value ( $\overline{\text{RMS}}$ ) of the surface shape error in three directions was taken as the optimized objective function. Consequently, the optimized objective functions in this paper were as follows:

$$\text{miny} = p(\mathbf{X}) = (p_1(\mathbf{X}), p_2(\mathbf{X})), \mathbf{X} \in \Omega \quad (5)$$

where  $\mathbf{X}$  is the optimization variable,  $\mathbf{X} = \{D_1, D_2, L_1, L_2\}$ ; and  $\Omega$  is the sample space.

$$p_1(\mathbf{X}) = \text{Mass}(D_1, D_2, L_1, L_2) \quad (6)$$

$$p_2(\mathbf{X}) = \overline{\text{RMS}} \quad (7)$$

where

$$\overline{\text{RMS}} = \frac{1}{3}(\text{RMS}_x(D_1, D_2, L_1, L_2) + \text{RMS}_y(D_1, D_2, L_1, L_2) + \text{RMS}_z(D_1, D_2, L_1, L_2)) \quad (8)$$

The parameters involved in the whole optimization process were the material properties of the mirror and the optimization parameters in the non-dominated sorting genetic algorithm. Table 1 lists all the parameter settings and the constraints for the optimized structural parameters.

During the process of finite-element analysis using Abaqus, a tetrahedral mesh type was adopted, and meshes were generated automatically by the software. In order to ensure accuracy of the results, the mesh size needed to be controlled. Here, the global size of mesh was less than 5 mm. In addition, the working condition of concern was to apply 1 G gravity along the Y direction.

**Table 1.** Optimization Parameters.

<b>Mirror Material Properties</b>	
<b>Components</b>	<b>Value</b>
Density	2.7 g/cm <sup>3</sup>
Young's Modulus	70 Gpa
Poisson's Ratio	0.27
<b>NSGA parameters</b>	
Population size	20
Mutation probability	0.15
Cross probability	0.8
Number of iterations	35
<b>Structural parameter constraints</b>	
$D_1$	[60, 80]
$D_2$	(0, $D_1 - 10$ ]
$L_1$	[0, 15]
$L_2$	[17.6, 22.6]

### 3.3. Optimization Results

Using the optimization method described in Section 2, the Pareto optimal solutions were obtained and are shown in Figure 4, where the circles represent optimization results obtained during iterations.

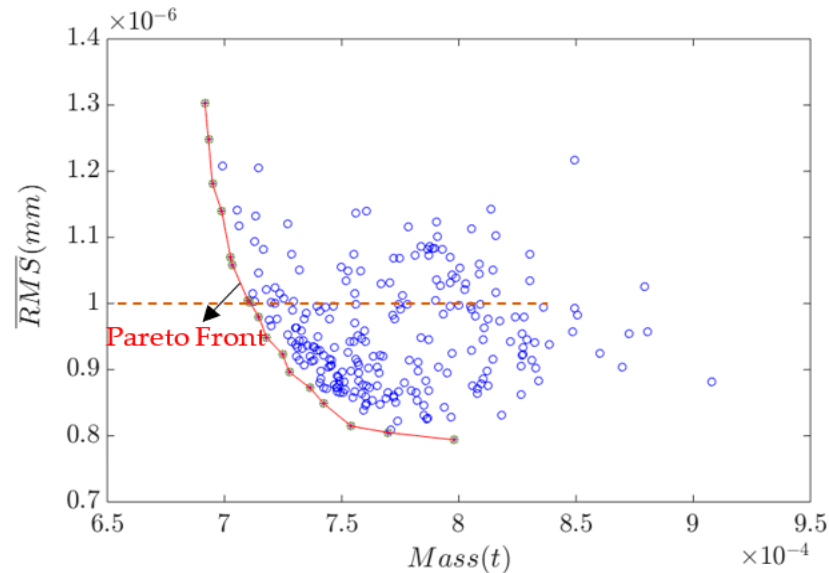


**Figure 4.** Pareto optimal solutions.

According to the obtained Pareto optimal solution set, the preferred optimal solution could be selected based on the weight of two objectives. In this case, the average surface shape error  $\overline{RMS}$  in the three directions was required to be less than 1 nm, and the total mass of the mirror was required to be as small as possible. Therefore,  $\overline{RMS} = 0.956$  nm and  $Mass = 717.9$  g was chosen in the optimal solution set as the final optimization solution. At this point, the surface shape error was obtained in three directions, respectively, as shown in Figures 5–7, and the optimization parameters as well as the specific optimization results are shown in Table 2. From the results in Table 1, we can see that although the average surface shape error was less than 1 nm, there were two components that were more than 1 nm, which were  $RMS_y$  and  $RMS_z$ . The surface shape error in the Y direction ( $RMS_y$ ) was the biggest of those in the three directions due to the effects of gravity. After removing the rigid-body motion, the aberrations in X direction were much smaller than those in the other two directions.

**Table 2.** Optimization results of the mirror.

Components	Value
$D_1$	64.4 mm
$D_2$	46 mm
$L_1$	13 mm
$L_2$	21.6 mm
$RMS_x$	$5.68 \times 10^{-7}$ mm
$RMS_y$	$1.24 \times 10^{-6}$ mm
$RMS_z$	$1.06 \times 10^{-6}$ mm
$\overline{RMS}$	$9.56 \times 10^{-7}$ mm
Mirror Mass	717.9 g

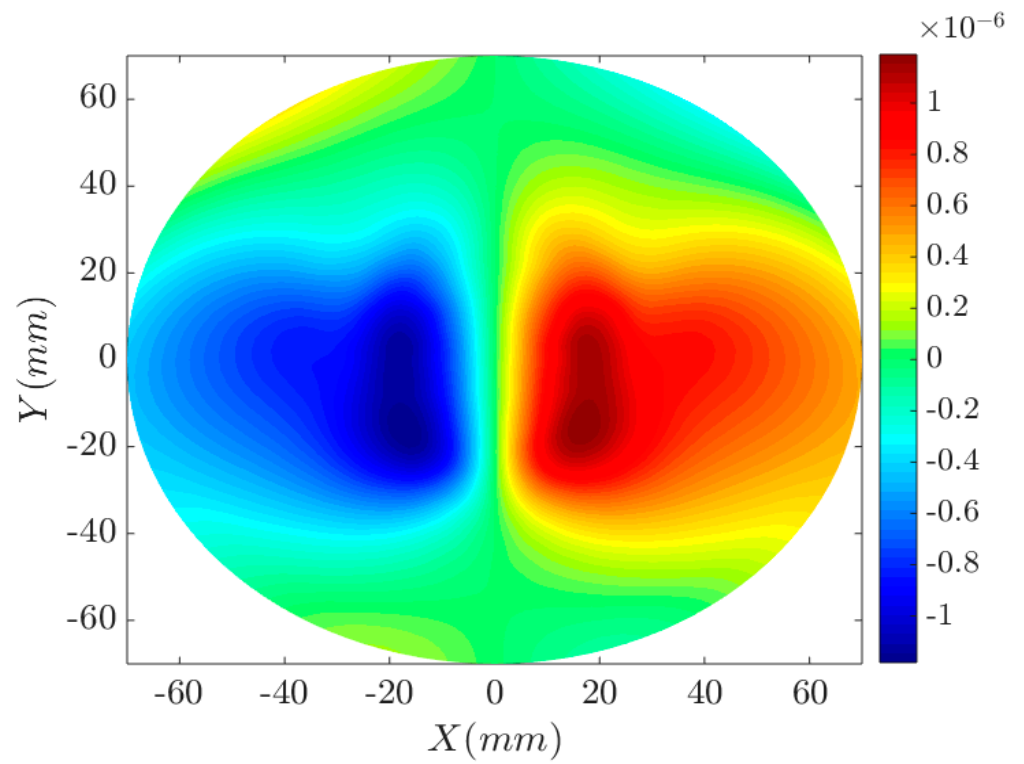


Figure 5. Surface shape error in X direction.

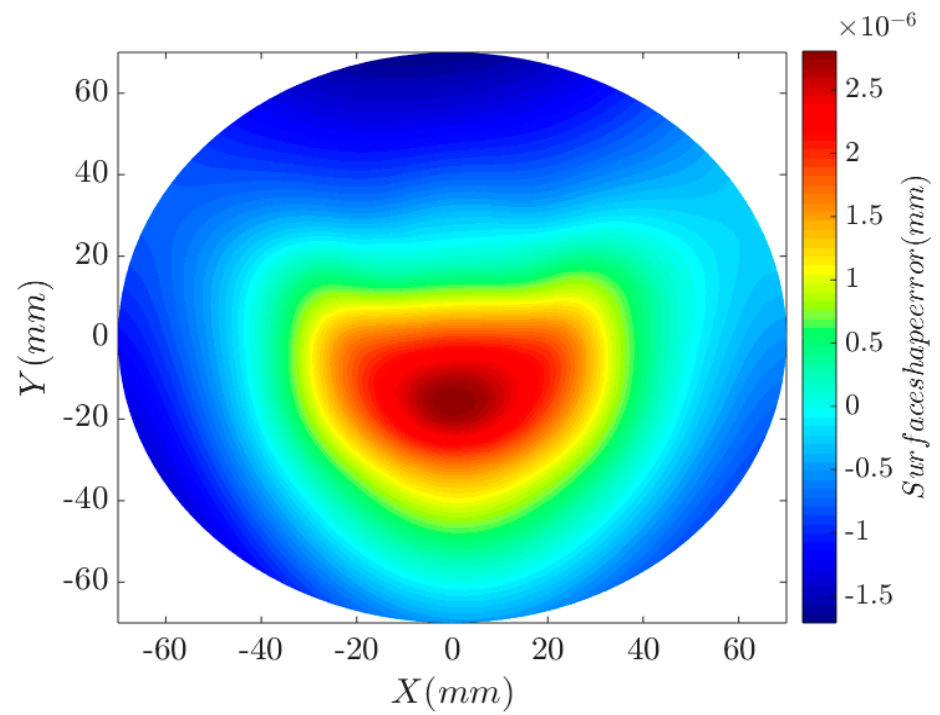
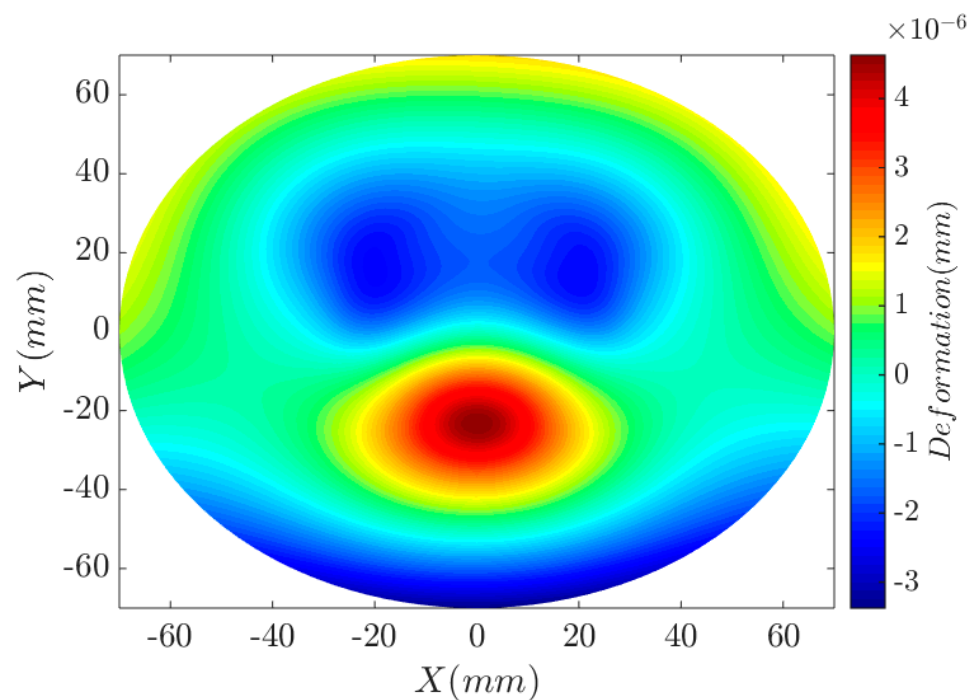


Figure 6. Surface shape error in Y direction.



**Figure 7.** Surface shape error in Z direction.

#### 4. Conclusions

The optimization design of mirror structures using the method proposed in this paper is conducive to realizing complex objective functions, which can help the design to meet designers' demands as well as avoid the problems of inefficient and ineffective optimization caused by changing the structure parameters manually. Moreover, compared with methods using optimization tools such as OptiStruct [2,7–9], it is not necessary to transform the multi-objective optimization problem into a single-objective optimization problem, and the interference of weight is excluded. In particular, this method could be flexibly combined with any advanced optimization algorithm and it is not limited to the built-in algorithms of the software used, which offers new ideas and possibilities to structural designers. In this paper, the optimization efficiency was improved by combining the population genetic superiority and inferiority characteristics in the non-dominated sorting genetic algorithm, and the Pareto optimal solution set was obtained for multi-objective optimization, which verified the effectiveness of this method. Future research will continue on the multi-objective optimization of mirror structures under more complex constraints and working conditions with advanced intelligent optimization algorithms.

**Author Contributions:** Conceptualization, L.S.; methodology, L.S.; software, L.S. and P.W.; validation, B.Z., Z.G. and P.H.; formal analysis, L.S.; investigation, Y.W.; resources, B.Z.; data curation, P.W.; writing—original draft preparation, L.S.; writing—review and editing, Z.G.; visualization, P.H.; supervision, B.Z.; project administration, Y.W.; funding acquisition, L.S. All authors have read and agreed to the published version of the manuscript.

**Funding:** This research was funded by the National Natural Science Foundation of China, grant number 62205337.

**Institutional Review Board Statement:** Not applicable.

**Informed Consent Statement:** Not applicable.

**Data Availability Statement:** Not applicable.

**Acknowledgments:** We thank for the support from the Key Laboratory of Airborne Optical Imaging and Measurement, Changchun Institute of Optics, Fine Mechanics and Physics, Chinese Academy of Sciences.

**Conflicts of Interest:** The authors declare that there are no conflicts of interest related to this article.

## References

- Bao, Q.W. Lightweight and Optimization Design and Research for the Opto-Mechanical Structure of Off-Axis Space Camera. Master's Thesis, University of Chinese Academy of Sciences, Beijing, China, 2016; p. 16.
- Liu, G.; Guo, L.; Wang, X.; Wu, Q. Topology and parametric optimization based lightweight design of a space reflective mirror. *Opt. Eng.* **2018**, *57*, 075101. [[CrossRef](#)]
- Jiang, C.; Miao, L.; Bao, Q.; Xie, Z.; Tan, Y.; Peng, Q.; Tan, Y. Optimized design of mirror support structure to reduce surface sensitivity. *Opt. Eng.* **2020**, *11*, 59. [[CrossRef](#)]
- Yang, J.W.; Huang, Q.L.; Han, Y.M. Application and Simulation in Fitting Optical Surface with Zernike Polynomial. *Spacecr. Recovery Remote Sens.* **2010**, *31*, 49–55.
- Wu, Q.W. Treating with surface figure error of mirror/lens by means of Surface equation. *Opt. Precis. Eng.* **1998**, *6*, 56–60.
- Zhang, C.; Li, Z. A Review of Lightweight Design for Space Mirror Core Structure: Tradition and Future. *Machines* **2022**, *10*, 1066. [[CrossRef](#)]
- Park, K.; Chang, S.; Youn, S. Topology optimization of the primary mirror of a multi-spectral camera. *Struct. Multidiscip. Optim.* **2003**, *25*, 46–53. [[CrossRef](#)]
- Sahu, R.; Patel, V.; Singh, S.K.; Munjal, B.S. Structural optimization of a space mirror to selectively constrain optical aberrations. *Struct. Multidiscip. Optim.* **2017**, *55*, 2353–2363. [[CrossRef](#)]
- Qu, Y.; Jiang, Y.; Feng, L.; Li, X.; Liu, B.; Wang, W. Lightweight Design of Multi-objective Topology for a Large-Aperture Space Mirror. *Appl. Sci.* **2018**, *8*, 2259. [[CrossRef](#)]
- Srinivas, N.; Deb, K. Multiobjective Function Optimization Using Nondominated Sorting Genetic Algorithms. *Evol. Comput.* **1994**, *2*, 1301–1308. [[CrossRef](#)]
- Deb, K. *Multi-Objective Optimization Using Evolutionary Algorithms*; John Wiley and Sons: Hoboken, NJ, USA, 2001.
- Deb, K.; Pratap, A.; Agarwal, S.; Meyarivan, T. A fast and elitist multi-objective genetic algorithm: NSGA-II. *IEEE Trans. Evol. Comput.* **2002**, *6*, 182–197. [[CrossRef](#)]
- Elarbi, M.; Bechikh, S.; Gupta, A.; BenSaid, L.; Ong, Y.S. A New Decomposition-Based NSGA-II for Many-Objective Optimization. *IEEE Trans. Syst. Man Cybern. Syst.* **2018**, *48*, 1191–1210. [[CrossRef](#)]
- Jian, H.; Xu, Y.; Chen, W.; Rang, T.; Tao, Z. An Improved NSGA-II Algorithm Based on Adaptive Weighting and Searching Strategy. *Appl. Sci.* **2022**, *12*, 11573.
- Xie, W.Z.; Li, Y.L.; Yang, S.Y. A Hybrid Multi-Objective Optimization Method and Its Application to Electromagnetic Device Designs. *Appl. Sci.* **2022**, *12*, 12110. [[CrossRef](#)]
- Deb, K.; Jain, H. An Evolutionary Many-Objective Optimization Algorithm Using Reference-Point-Based Nondominated Sorting Approach, Part I: Solving Problems with Box Constraints. *IEEE Trans. Evol. Comput.* **2013**, *18*, 577–601. [[CrossRef](#)]
- Granata, V.; Pierro, V.; Troiano, L. Meta-Heuristics Optimization of Mirrors for Gravitational Wave Detectors: Cryogenic Case. *Appl. Sci.* **2022**, *12*, 7680. [[CrossRef](#)]
- Dhanalakshmi, S.; Kannan, S.; Mahadevan, K.; Baskar, S. Application of modified NSGA-II algorithm to combined economic and emission dispatch problem. *Int. J. Electr. Power Energy Syst.* **2011**, *33*, 992–1002. [[CrossRef](#)]
- Baklouti, A.; Dammak, K.; Hami, A.E. Optimum reliable design of rolling element bearings using multi-objective optimization based on C-NSGA-II. *Reliab. Eng. Syst. Saf.* **2022**, *223*, 108508. [[CrossRef](#)]
- Zangoeei, M.H.; Habibi, J.; Alizadehsani, R. Disease Diagnosis with a hybrid method SVR using NSGA-II. *Neurocomputing* **2014**, *136*, 14–29. [[CrossRef](#)]
- Kurita, M.; Ohmori, H.; Kunda, M.; Kawamura, H.; Noda, N.; Seki, T.; Nishimura, Y.; Yoshida, M.; Sato, S.; Nagata, T. Light-weight telescope structure optimized by genetic algorithms. *Proc. SPIE* **2010**, *7733*, 54–58.
- Kihm, H.; Yang, H.S.; Moon, I.K.; Yeon, J.H.; Lee, S.H.; Lee, Y.W. Adjustable bipod flexures for mounting mirrors in a space telescope. *Appl. Opt.* **2012**, *51*, 76–83. [[CrossRef](#)] [[PubMed](#)]
- Kihm, H.; Yang, H. Design optimization of a 1-m lightweight mirror for a space telescope. *Opt. Eng.* **2013**, *52*, 091806. [[CrossRef](#)]
- Zhang, X.; Sun, L.; Qi, L. Bayesian Regularization Algorithm Based Recurrent Neural Network Method and NSGA-II for the Optimal Design of the Reflector. *Machines* **2022**, *10*, 63. [[CrossRef](#)]
- Zhang, Y.; Ding, Z.; Zhao, H.J.; Zou, B.Y. Rigid-body displacement separation of optics in optical-structural-thermal integrated analysis. *Infrared Laser Eng.* **2012**, *41*, 276.
- Zhang, J.Q.; Dong, D.Y.; Wu, Q.W.; Yan, C.X.; Zhang, X.J. Treatment of surface figure error and rigid body motion for mirror/lens in optical remote sensor. *Chin. J. Sci. Instrum.* **2011**, *32*, 242–247.
- Doyle, K.B.; Genberg, V.L.; Michels, G.J. Chapter 4: Optical surface error. In *Integrated Optomechanical Analysis*, 2nd ed.; National Defense Industry Press: Beijing, China, 2015; pp. 67–76.

28. Tan, S.L.; Wang, L.J.; Zhang, X.; Zhang, J.Z.; Xie, X.L. Snap Together Design and Analysis of Visible Quality Aluminum Mirror. *J. Chang. Univ. Sci. Technol.* **2017**, *40*, 5–12.
29. Zhang, J.Z.; Zhang, X.; Tan, S.L.; Xie, X.L. Design and Manufacture of an Off-axis Aluminum Mirror for Visible-light Imaging. *Curr. Opt. Photonics* **2017**, *1*, 364–371.
30. Wu, J.F. Design of High-lightweight Space Mirror Component Based on Automatic Optimization. *J. Phys. Conf. Ser.* **2020**, *1605*, 012023. [[CrossRef](#)]

**Disclaimer/Publisher’s Note:** The statements, opinions and data contained in all publications are solely those of the individual author(s) and contributor(s) and not of MDPI and/or the editor(s). MDPI and/or the editor(s) disclaim responsibility for any injury to people or property resulting from any ideas, methods, instructions or products referred to in the content.